

A high-performance, tailor-made resolving agent: remarkable enhancement of resolution ability by introducing a naphthyl group into the fundamental skeleton^{1 † ‡}

2 PERKIN

Kazushi Kinbara,§ Yoshiko Harada and Kazuhiko Saigo* §

Department of Chemistry and Biotechnology, Graduate School of Engineering,
The University of Tokyo, Hongo, Bunkyo-ku, Tokyo 113-8656, Japan

Received (in Cambridge, UK) 2nd February 2000, Accepted 23rd May 2000

Published on the Web 15th June 2000

A novel resolving agent, 2-naphthylglycolic acid (2-NGA), was designed for *p*-substituted 1-arylethylamines on the basis of the consideration that a rigid and large naphthyl group would be favorable for the close packing of supramolecular hydrogen-bond sheets formed between the carboxy groups of 2-NGA and the amino groups of *p*-substituted 1-arylethylamines. Racemic 2-NGA was readily available from commercially available raw materials, and both enantiopure forms could be obtained by simple diastereomeric resolution with enantiopure 1-phenylethylamine. Thus-prepared enantiopure 2-NGA was found to have an excellent resolution ability not only for *p*-substituted 1-arylethylamines, but also for a wide variety of chiral primary amines. X-Ray crystallographic analyses of the less- and more-soluble diastereomeric salts revealed that this excellent resolution ability of 2-NGA arose from the formation of a supramolecular hydrogen-bond sheet with the primary amine, as we had expected, and also from the possible achievement of an infinite chain of CH $\cdots\pi$ interaction between its naphthyl group and the aromatic group of the amine, which was formed in the hydrophobic region of the supramolecular hydrogen-bond sheet.

Introduction

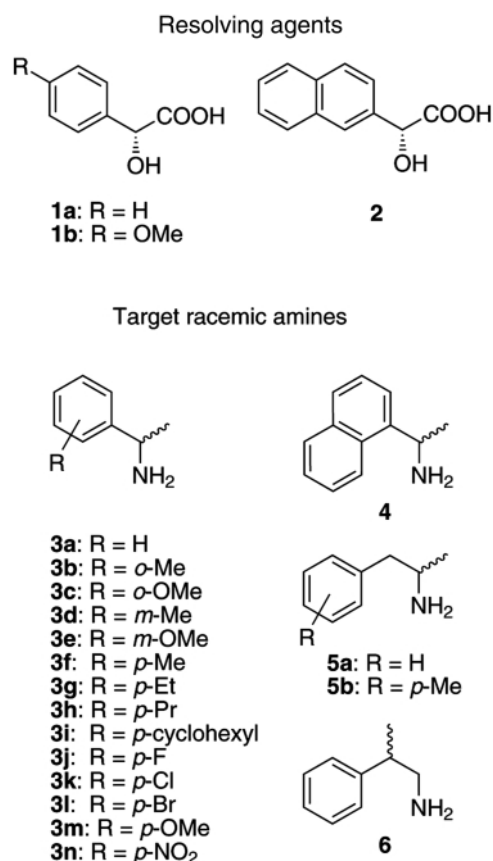
The optical resolution of enantiomers *via* the formation of the corresponding diastereomeric salts, so-called classical resolution, is widely used for laboratory-scale separations as well as for the preparation of pharmaceuticals and agrochemicals on an industrial scale.² Although nearly 150 years have passed since this diastereomeric salt method was developed by Pasteur,³ the method still involves serious problems, because much trial-and-error is required in order to choose a suitable resolving agent, and because complete resolution is not necessarily accomplished with known resolving agents. Therefore, the *ab initio* prediction and/or design of an appropriate resolving agent for a given target racemate is a challenging goal in the development of this important method.

In order to understand the mechanism of diastereomeric resolution by crystallisation, recent studies have clarified the important physical properties of diastereomeric-salt mixtures by identifying the types of diastereomeric-salt mixtures,² utilising their phase diagrams for solid-liquid equilibria,⁴ estimating the thermodynamic stability of the less- and more-soluble diastereomeric salts,⁵ *etc.* On the other hand, from the viewpoint of the molecular design of a resolving agent, it is particularly important to clarify the relationship between the above-mentioned physical properties of pairs of diastereomeric salts and the characteristics of their molecular and/or crystal structures.⁶

[†] In memory of Professor Dr André Collet.

[‡] Table S1 (N \cdots O and O \cdots O distances in the diastereomeric salts of enantiopure **2** with **3**) and Table S2 (shortest H \cdots C distances between the aromatic group of the ammonium molecule (A) and those of the carboxylate molecules (B-E)) are available as supplementary data. For direct electronic access see <http://www.rsc.org/suppdata/p2/b0/b000903m/>

§ Present address: Department of Integrated Biosciences, Graduate School of Frontier Sciences, The University of Tokyo, Hongo, Bunkyo-ku, Tokyo 113-8656, Japan.



Taking this situation into account, we have been undertaking systematic studies on diastereomeric resolution and attempting to establish a criterion for the design of tailor-made resolving agents, especially from the viewpoint of crystal engineering.⁷⁻⁹ During the course of our studies, we found that in the case of the resolution of 1-arylethylamines by mandelic acid (**1a**), a

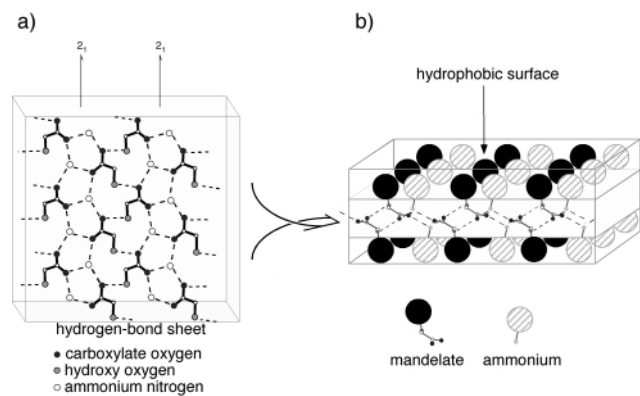


Fig. 1 Schematic representations of the hydrogen-bond network formed in the less-soluble salts of enantiopure mandelic acid with 1-arylethylamines. a) Viewed down the supramolecular hydrogen-bond sheet. b) Edge-on view of the supramolecular hydrogen-bond sheet.

quite characteristic supramolecular hydrogen-bond sheet, the surfaces of which were planar and favorable for close packing, was commonly formed in the *less-soluble* salts, when high efficiency of resolution was achieved (Fig. 1);⁹ all of the less-soluble salts were commonly stabilised by two kinds of interactions, hydrogen-bonding and van der Waals interactions. On the other hand, the crystal structures of the corresponding *more-soluble* salts showed versatility, and such a stable structure has not been achieved in the crystals. From these results, it was suggested that for the development of a new resolving agent, one should design it to make the less-soluble salt with a racemate as stable as possible; a study on the system of mandelic acid–1-arylethylamine indicated that the complementarity in molecular length between the resolving agent and the racemate was important for achieving such a stable packing of supramolecular sheets in the *less-soluble* salts. On the basis of this criterion, we designed *p*-methoxymandelic acid (**1b**), which has a molecular length complementary with *p*-substituted 1-arylethylamines, and found that **1b** had a distinctively higher resolution ability than **1a** for these amines.^{8,9} However, the results of the resolutions by **1b** were not satisfactory from the viewpoint of practical use.

We then tried to design a more powerful and practical resolving agent for these amines by introducing a more effective functional group, which was expected to affect the chiral discrimination upon stabilising less-soluble salts, into the resolving agent, following the above-mentioned criterion. A candidate for such a resolving agent is 2-naphthylglycolic acid (**2**), which was designed on the basis of the following considerations: (1) Since it was considered that the flexibility of the substituent on the *p*-position of the aromatic ring of **1b** would make its molecular length ambiguous and diminish the efficiency of the packing of supramolecular sheets, a compound having a rigid skeleton would be appropriate as a resolving agent.¹⁰ (2) From the viewpoint of the close packing of molecules in an individual supramolecular sheet, *i.e.* its stability, the resolving agent should have not only an appropriate molecular length, but also an appropriate volume, which could fill the vacant space close to the surface of the supramolecular sheet upon elongating the molecular length. (3) In some cases, a naphthyl group contributes to stabilisation of the crystal packing through the formation of CH $\cdots\pi$ or $\pi\cdots\pi$ interaction,¹¹ indicating that a third factor, CH $\cdots\pi$ or $\pi\cdots\pi$ interaction, may be considered for the explanation of the discrimination mechanism. Finally, we designed **2**, which has a 2-naphthyl group in the place of the phenyl group of **1a**, as a novel resolving agent in the present study.

Here, we describe the preparation and application of a novel tailor-made resolving agent **2** to the resolution of 1-arylethylamines including *p*-substituted ones, and discuss important

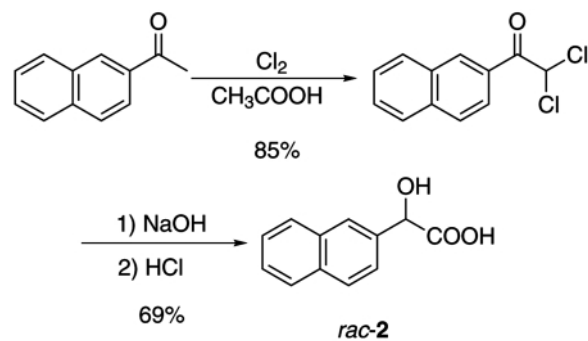
factors that influence the chiral discrimination during crystallisation.

Results and discussion

Preparation of enantiopure 2-naphthylglycolic acid

Although some procedures have been reported for the preparation of optically active **2**,^{12–14} they could not be applied to the synthesis of its enantiopure form on a practical scale. We then tried to develop a new method for the practical-scale preparation of enantiopure **2**.

At first, the synthesis of racemic **2** was examined and could be accomplished by following the procedure reported for the synthesis of mandelic acid (Scheme 1);¹⁵ racemic **2** could be



Scheme 1

obtained in an acceptable yield (overall 59%) by dichlorination of commercially available 2-acetonaphthone, followed by hydrolysis and intramolecular oxidation–reduction. For a large-scale preparation of racemic **2**, this method was found to be more convenient than other known procedures from the viewpoints of easy handling and low cost.^{16,17}

Then, the resolution of racemic **2** was studied by using enantiopure 1-phenylethylamine, 1-(*p*-tolyl)ethylamine, and *erythro*-2-amino-1,2-diphenylethanol as resolving agents.^{18,19} As a result, (*R*)- or (*S*)-1-phenylethylamine (**3a**), which can be obtained commercially in large quantities, was found to be the most effective agent for the resolution of racemic **2**. Recrystallisation of **2**·(*R*)-**3a** salt, prepared from a 1:1 mixture of racemic **2** and (*R*)-**3a**, from 90% aqueous ethanol three times gave pure (*R*)-**2**·(*R*)-**3a** salt in 28% overall yield (Scheme 2). The treatment of (*R*)-**2**·(*R*)-**3a** salt with hydrochloric acid afforded crystalline crude (*R*)-**2**, which was further purified by recrystallisation from chloroform–ethanol to give enantiopure (*R*)-**2** in 25% overall yield. In a similar manner, enantiopure (*S*)-**2** could also be obtained by repeated recrystallisations (three times) of the salt of (*S*)-enriched **2**, recovered from the filtrate of the first recrystallisation of the (*R*)-**2**·(*R*)-**3a** salt, with (*S*)-**3a**.

Resolution ability of enantiopure **2** for 1-arylethylamines

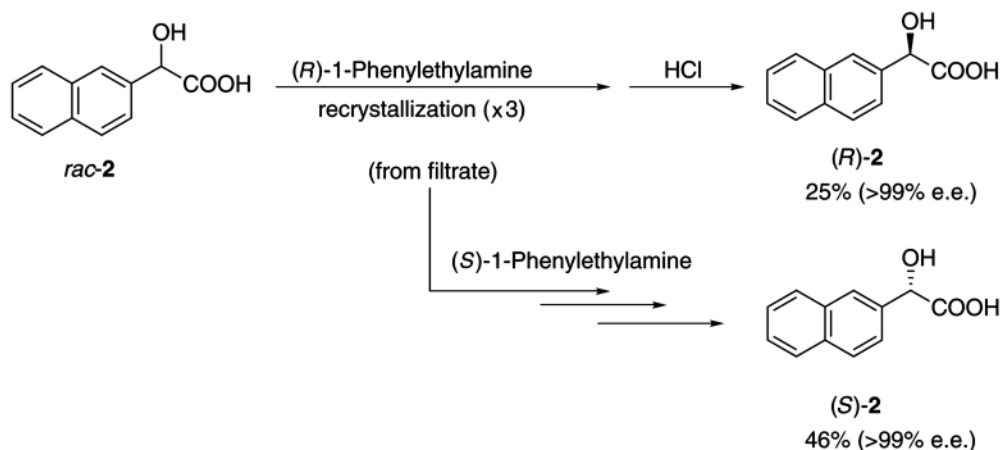
The resolution of various *p*-substituted 1-arylethylamines as well as other types of chiral amines was performed using enantiopure **2** as a resolving agent. The results are summarised in Table 1. The yield in Table 1 is based on the half amount of the racemate. In order to make the crystallisation conditions as similar as possible and to avoid the problem of polymorphs, crystallisation was performed only once from aqueous ethanol at a constant temperature (30 °C). The ratio of ethanol:water and the amount of the solvent were adjusted so as to control the yield of the precipitated salt to be as close as possible to the range of 50–80%.

As can be seen from Table 1, enantiopure **2** has an excellent resolving ability over a range of amines. In the case of the resolution of **3k** (entry 11), which is a valuable intermediate for pharmaceuticals, an additional recrystallisation, for example,

Table 1 Resolution of chiral amines 3–6 with enantiopure 2^a

Entry	Racemic amine	Absolute configuration of 2	Solvent ratio (EtOH:H ₂ O) ^b	Yield (%) ^c	Ee (%) ^d	Yield × ee	Absolute configuration of major enantiomer
1	3a	R	2.0:0.04	61	96	0.59	R
2	3b	S	2.0:0.15	76	7	0.05	R
3	3c	S	—	— ^e	—	—	—
4	3d	S	1.0:1.25	40	98	0.39	S ^f
5	3e	S	1.8:0.2	68	98	0.67	S
6	3f	R	4.2:0.4	81	95	0.77	R
7	3g	S	4.2:1.2	62	>99	0.61	S
8	3h	S	5.0:0.5	80	>99	0.79	S ^f
9	3i	S	8.5:1.5	50	91	0.46	S ^f
10	3j	S	1.4:0.2	69	94	0.65	S ^f
11	3k	S	5.0:1.1	77	98	0.75	S
12	3l	S	4.4:2.5	81	93	0.75	S
13	3m	R	1.5:0.25	58	87	0.50	R
14	3n	S	2.0:0.2	70	88	0.56	S
15	4	S	6.0:0.6	73	>99	0.72	S
16	5a	S	3.6:0.09	96	48	0.46	— ^g
17	5b	R	6.7:0	68	4	0.03	— ^g
18	6	S	4.0:0.13	91	69	0.63	— ^g

^a The resolution was carried out on a 1–3 mmol-scale. ^b The weight (g) of the solvent normalized to a 1 mmol-scale. ^c Yield of the crystallized diastereomeric salt based on a half amount of the racemic amine. ^d Enantiomeric excess (ee) of the liberated amine, which was determined by an HPLC analysis [Daicel CrownPak CR(+) (entries 1, 3–14 and 16–18) and Chiralcel OJ-R (entries 2 and 15)]. ^e Not crystallized. ^f Deduced from the order of elution in the HPLC analysis. ^g Not determined.



afforded diastereomerically pure (*S*)-2·(*S*)-3k (67% overall yield).²⁰ The complete resolution of 4 could also be accomplished by only one additional recrystallisation (53% overall yield).²¹ In each case, the absolute configuration of the amines in the less-soluble salts correlated with that of 2 used, *i.e.*, the (*S*)-enantiomer was obtained as a major isomer when (*S*)-2 was used, and *vice versa*. It is noteworthy that even an amine having a largely bulky substituent on the *p*-position, which apparently has a longer molecular length than that of 2 (entry 9), as well as *m*- and non-substituted amines, which apparently have a shorter molecular length than that of 2 (entries 1, 4, and 5), could be efficiently resolved by enantiopure 2; it seems that the relative molecular length is a less important factor in the case of the resolution of 1-arylethylamines by enantiopure 2. In addition, even when a group capable of strong hydrogen-bond formation, such as a nitro group, was present on the aromatic group of an amine, the efficiency of resolution remained very high (entry 14). Since a slight change in the molecular structure of a racemate usually exerts a dramatic effect on the efficiency of resolution, this consistent and excellent resolving ability of enantiopure 2 for such a wide variety of amines is remarkable.

Enantiopure 2 was also effective for the resolution of 2-arylalkylamine 5a and β-chiral amine 6 (entries 16 and 18). However, when a substituent which elongated the molecular

length of an amine was introduced on the aromatic group of 5a, the efficiency of resolution was dramatically diminished (entry 17). This result indicates that the relative molecular length still plays some role in achieving high efficiency of resolution.

Binary melting point phase diagrams of the diastereomeric salts

Success in diastereomeric resolution is influenced by a number of factors. Particularly, the identification of the type of diastereomeric-salt mixtures is valuable in order to understand the chiral discrimination mechanism and to optimise the resolution conditions. Diastereomeric-salt mixtures are classified into three types: a eutectic mixture, a 1:1 addition compound, and a solid solution, which could be distinguished from each other on the basis of the binary melting point phase diagram of the diastereomeric-salt mixtures.²

Fig. 2 shows binary melting-point phase diagrams for a mixture of (*R*)-2·3f, (*S*)-2·3k, and (*S*)-2·4. Phase diagrams calculated using the Schröder–van Laar equation²² are also shown in Fig. 2. As shown in Fig. 2, each system is a eutectic mixture, and the eutectic composition lies toward the end of the diagram, resulting in an almost ideal efficiency and yield. The resolution efficiency (*S*) can be calculated using eqn. (1),²

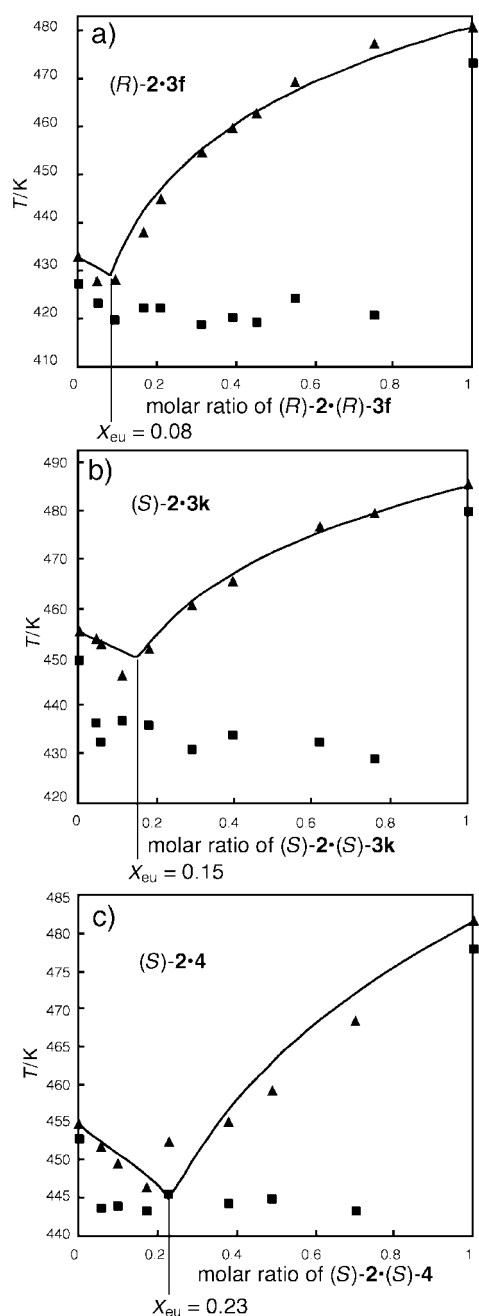


Fig. 2 Binary melting-point phase diagrams for a) (R) - $2 \cdot 3f$, b) (S) - $2 \cdot 3k$, and c) (S) - $2 \cdot 4$. The squares and triangles represent the temperatures of start and end of melting, respectively. The solid curve represents the calculated values on the basis of the Schröder–van Laar equation.

$$S = \frac{1 - 2x_{eu}}{1 - x_{eu}} \quad (1)$$

where x_{eu} is the eutectic composition. As a result, resolution efficiencies (S) were estimated to be 0.91, 0.81, and 0.70 for (R) - $2 \cdot 3f$, (S) - $2 \cdot 3k$, and (S) - $2 \cdot 4$, respectively. These results indicate that the values of yield \times ee in Table 1 are meaningful, since they are close to the calculated resolution efficiencies for each system.

The fact that the system is a eutectic mixture indicates that the resolution efficiency primarily depends on the difference in stability between the less- and more-soluble salts. Table 2 gives some of the physical parameters of the less- and more-soluble salts of (R) - $2 \cdot 3f$, (S) - $2 \cdot 3k$, and (S) - $2 \cdot 4$. As can be seen from Table 2, it is strongly suggested that the less-soluble salt is thermodynamically much more stable than the corresponding more-soluble salt for each case. We then focused on the crystal

Table 2 Melting point, fusion enthalpy, and solubility of selected less- and more-soluble salts

Salt	Mp/K	$\Delta H_{fus}/$ kJ mol ⁻¹ ^a	Solubility ^b
(R) - $2 \cdot (R)$ - $3f$ (less)	491.5–493.5	82.4	0.84
(R) - $2 \cdot (S)$ - $3f$ (more)	428.0–430.5	37.5	5.74
(S) - $2 \cdot (S)$ - $3k$ (less)	481.5–485.0	96.5	0.70
(S) - $2 \cdot (R)$ - $3k$ (more)	444.0–447.0	53.2	1.57
(S) - $2 \cdot (S)$ - 4 (less)	477.0–479.0	71.2	0.80
(S) - $2 \cdot (R)$ - 4 (more)	453.0–455.0	48.4	3.11

^a Determined by a DSC analysis. ^b Weight (g) of the solute dissolved in 100 g of 95% aqueous ethanol.

structure of the less- and more-soluble salts in the next stage in order to find which property of the crystal of the diastereomeric salt is correlated to the difference in stability and why such high resolution ability of enantiopure **2** is achieved over a variety of amines.

Comparison of crystal structures of the less- and more-soluble salts

In the present study, we could determine the crystal structures of six less-soluble salts and three more-soluble salts (Table 3). Just as we expected at the beginning of the present study, in all of the crystals of six less-soluble salts, there commonly exist quite tightly hydrogen-bonded supramolecular sheets, as were found in the less-soluble salts of **1a** and **1b** with 1-arylethylamines (Fig. 3).²³ In addition, similar hydrogen-bond sheets were also formed in the corresponding more-soluble salts. On the other hand, the hydrophobic surfaces of the supramolecular hydrogen-bond sheet are planar in each less- and more-soluble salt, so as to realise a close packing of these sheets. The naphthyl group of **2** efficiently fills the hydrophobic region in the supramolecular sheet and makes the surfaces of the supramolecular sheet planar in each less- and more-soluble salt. It is noteworthy that, in addition to these two characteristics, there exists an additional characteristic in these less- and more-soluble salts; a herringbone packing²⁴ is realised between the naphthyl groups of **2**-anions and the aryl groups of the ammonium cations in the hydrophobic region of the supramolecular hydrogen-bond sheet.

Fig. 4a shows the packing of the aromatic rings at the hydrophobic surface of the supramolecular hydrogen-bond sheet in (R) - $2 \cdot (R)$ - $3f$. In the less-soluble salts and more-soluble (S) - $2 \cdot (R)$ - $3g$ and (S) - $2 \cdot (R)$ - $3k$ salts, the aromatic group of the ammonium molecule **A** is stabilised by $CH \cdots \pi$ interactions with four surrounding naphthyl groups of **2**-anions (B–E).^{11,25} Subsequently, an infinite layer of $CH \cdots \pi$ interactions is realised in the hydrophobic region of the supramolecular hydrogen-bond sheet as shown in Fig. 4b. Such an infinite web of $CH \cdots \pi$ interactions was not attained at all in the previously reported less-soluble salts of mandelic acid and *p*-substituted mandelic acids with 1-arylethylamines. This means that the formation of an infinite layer of $CH \cdots \pi$ interaction is a notable characteristic of the salts of enantiopure **2** with 1-arylethylamines.

Thus, the crystal structures of the less- and more-soluble salts are essentially similar to each other; three kinds of interactions, *viz.* hydrogen-bonding, $CH \cdots \pi$, and hydrophobic interactions, play important roles in stabilisation of the crystals. As is mentioned above, among these three interactions, the hydrophobic interaction, which is correlated with the planarity of the hydrophobic surface of the supramolecular sheet, is not a major factor determining the difference in stability between the less- and more-soluble salts, unlike the previously reported mandelic acid salts. We then focused our attention on the detailed structure of an individual supramolecular sheet formed in these salts.

Table 3 Summary of the crystal data of the diastereomeric salts of enantiopure **2** with 1-arylethylamines

Compound	(<i>R</i>)- 2 ·(<i>R</i>)- 3a (less soluble)	(<i>S</i>)- 2 ·(<i>S</i>)- 3e (less soluble)	(<i>R</i>)- 2 ·(<i>R</i>)- 3f (less soluble)	(<i>S</i>)- 2 ·(<i>S</i>)- 3g (less soluble)	(<i>S</i>)- 2 ·(<i>S</i>)- 3k (less soluble)	(<i>R</i>)- 2 ·(<i>R</i>)- 3m (less soluble)	(<i>R</i>)- 2 ·(<i>S</i>)- 3f (more soluble)	(<i>S</i>)- 2 ·(<i>R</i>)- 3g (more soluble)	(<i>S</i>)- 2 ·(<i>R</i>)- 3k (more soluble)
Formula	C ₂₀ H ₂₁ NO ₃	C ₂₁ H ₂₃ NO ₄	C ₂₁ H ₂₃ NO ₃	C ₂₂ H ₂₅ NO ₃	C ₂₀ H ₂₀ NO ₃ Cl	C ₂₁ H ₂₃ NO ₄	C ₂₁ H ₂₃ NO ₃	C ₂₂ H ₂₅ NO ₃	C ₂₀ H ₂₀ NO ₃ Cl
Formula weight	323.40	353.40	337.40	351.4	357.80	353.40	337.40	351.4	357.80
Crystal system	Monoclinic	Orthorhombic	Orthorhombic	Monoclinic	Orthorhombic	Orthorhombic	Monoclinic	Monoclinic	Orthorhombic
Space group	<i>C</i> 2	<i>P</i> 2 ₁ 2 ₁ 2 ₁	<i>P</i> 2 ₁ 2 ₁ 2 ₁	<i>P</i> 2 ₁	<i>P</i> 2 ₁ 2 ₁ 2 ₁	<i>P</i> 2 ₁ 2 ₁ 2 ₁	<i>C</i> 2	<i>P</i> 2 ₁	<i>P</i> 2 ₁ 2 ₁ 2 ₁
<i>a</i> /Å	30.573(7)	8.342(1)	8.412(2)	16.625(5)	8.420(2)	8.673(2)	33.84(1)	16.81(1)	8.611(1)
<i>b</i> /Å	6.835(2)	32.625(5)	31.505(6)	6.757(3)	31.089(6)	31.12(1)	5.952(3)	6.430(2)	31.413(4)
<i>c</i> /Å	8.446(2)	6.893(2)	6.869(1)	8.507(3)	6.869(2)	6.872(2)	9.227(3)	8.945(4)	6.754(1)
<i>a</i> '°	90	90	90	90	90	90	90	90	90
<i>β</i> '°	100.26(2)	90	90	91.38(3)	90	90	93.36(3)	95.80(4)	90
<i>γ</i> '°	90	1875.9(6)	1820.3(6)	955.3(5)	1789.1(6)	1855.0(9)	1855.1(1)	961.7(8)	1826.9(5)
<i>V</i> /Å ³	1736.6(9)	4	4	2	4	4	4	2	4
<i>Z</i>	4	4	4	2	4	4	4	2	4
<i>d</i> /mm ⁻¹	0.667	0.702	0.657	0.645	2.032	0.710	0.644	0.640	2.000
Temperature/K	293	293	293	293	293	293	293	293	293
Measured reflections	1603	1485	1424	1638	1690	1655	1615	1829	1743
Independent reflections	1367	1312	1380	1433	1524	1443	1471	1362	1532
<i>R</i> _{int}	0.035	0.086	0.050	0.067	0.022	0.026	0.034	0.069	0.081
<i>R</i>	0.061	0.053	0.094	0.072	0.068	0.075	0.059	0.098	0.101

As a result, an obvious difference is observed in the location of the hydroxy group of **2**-anion upon comparison of less-soluble (*S*)-**2**·(*S*)-**3g** with more-soluble (*S*)-**2**·(*R*)-**3g**, and less-soluble (*S*)-**2**·(*S*)-**3k** with more-soluble (*S*)-**2**·(*R*)-**3k**; the relative position of the α -hydrogen and hydroxy group of **2**-anion in the more-soluble salts is opposite to that in the less-soluble salts (Fig. 3a and b). This causes a difference in the mode of hydrogen-bonding; in the less-soluble salts, the hydroxy oxygen of **2**-anion forms bifurcated hydrogen bonds with the carboxylate oxygen and the ammonium hydrogen as shown in Fig. 5a, while in the more-soluble salts, the usual one-dimensional hydrogen bonds are formed since the oxygen is apart from the ammonium hydrogen (Fig. 5b). In addition, the difference in the infrared absorption band arising from the hydroxy and the carboxylate groups between the more- and less-soluble salts suggests that only a much weaker hydrogen-bonding interaction exists in the more-soluble salt.^{26,27} Therefore, it is considered that in more-soluble (*S*)-**2**·(*R*)-**3g** and (*S*)-**2**·(*R*)-**3k**, the supramolecular sheet is less stable from the viewpoint of a hydrogen-bonding interaction than the corresponding less-soluble salts.

On the other hand, the modes of the packing of the aromatic groups are rather different from each other between less-soluble (*R*)-**2**·(*R*)-**3f** and more-soluble (*R*)-**2**·(*S*)-**3f** (Fig. 6). In the less-soluble salt, the aromatic groups are rather vertical to the surface of the supramolecular sheet, and a quite compact packing of the aromatic groups is achieved (Fig. 6a). On the other hand, in the more-soluble (*R*)-**2**·(*S*)-**3f**, the aromatic groups are somewhat inclined toward the surface of the supramolecular sheet (Fig. 6b). Moreover, in the less-soluble salt, the interplanar angle between the aromatic groups is 84°, which is close to the ideal angle (90°)²⁸ for efficient CH... π interaction, while the angle in the case of more-soluble (*R*)-**2**·(*S*)-**3f** is 54°, which is far from the ideal angle. Thus the packing of the aromatic groups at the hydrophobic surfaces of the supramolecular sheets in more-soluble (*R*)-**2**·(*S*)-**3f** would be less favorable than that in the corresponding less-soluble (*R*)-**2**·(*R*)-**3f** from the viewpoint of CH... π interaction.

These results suggest that the difference in the magnitude of the hydrogen-bonding interaction and/or CH... π interaction in the supramolecular hydrogen-bond sheet between the less- and more-soluble salts makes the difference in stability between the less- and more-soluble salts sufficient for efficient chiral discrimination. Moreover, it is indicated that for the resolution of 1-arylethylamines with **2**, the close packing of a supramolecular sheet in the less-soluble salts would be a less important factor for their successful resolution. This interpretation is in accordance with the results given in Table 1 that the efficiency in the resolution of 1-arylethylamines by enantiopure **2** is not affected by the relative molecular length between them.

On the other hand, the results in Table 1 also suggest that for chiral 2-arylalkylamines, such as **5a**, **5b**, and **6**, enantiopure **2** had a significantly lower resolution ability than for 1-arylethylamines. In the cases of these 2-arylalkylamines, the aromatic group is located in a different position and situated in a different orientation from that of 1-arylethylamines in a supramolecular sheet. This would cause less-efficient CH... π interaction in the crystals and insufficient stabilisation of the supramolecular sheet. In such a case, hydrophobic interaction between the hydrogen-bonded sheets would be a significant factor for the stabilisation of the less-soluble diastereomeric salts just like the cases of previously studied mandelic acid salts;⁹ in such cases, the relative molecular length of the racemates would become important for achieving high resolution efficiency.

Conclusions

Upon introducing a naphthyl moiety into an enantiopure α -hydroxy acid, its resolution ability for *p*-substituted 1-aryl-

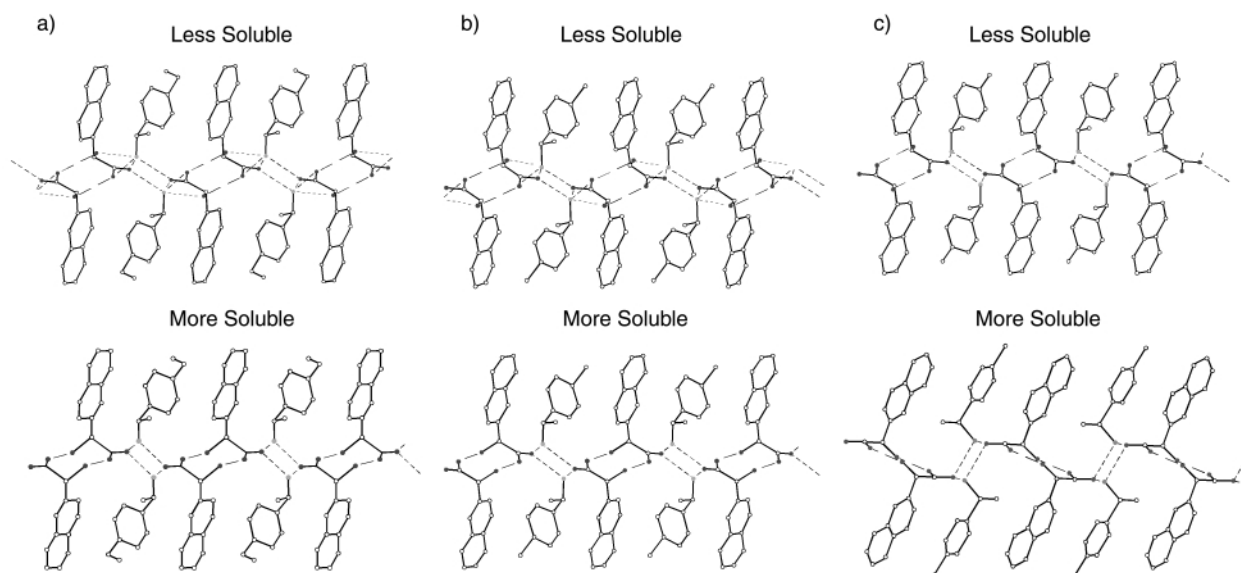


Fig. 3 The edge-on view of the supramolecular hydrogen-bond sheet in the less- and more-soluble salts. a) Less-soluble (*S*)-2·(*S*)-3g and more-soluble (*S*)-2·(*R*)-3g. b) Less-soluble (*S*)-2·(*S*)-3k and more-soluble (*S*)-2·(*R*)-3k. c) Less-soluble (*R*)-2·(*R*)-3f and more-soluble (*R*)-2·(*S*)-3f. The hydrogen atoms are omitted for clarity. The dotted lines show the hydrogen bonds.

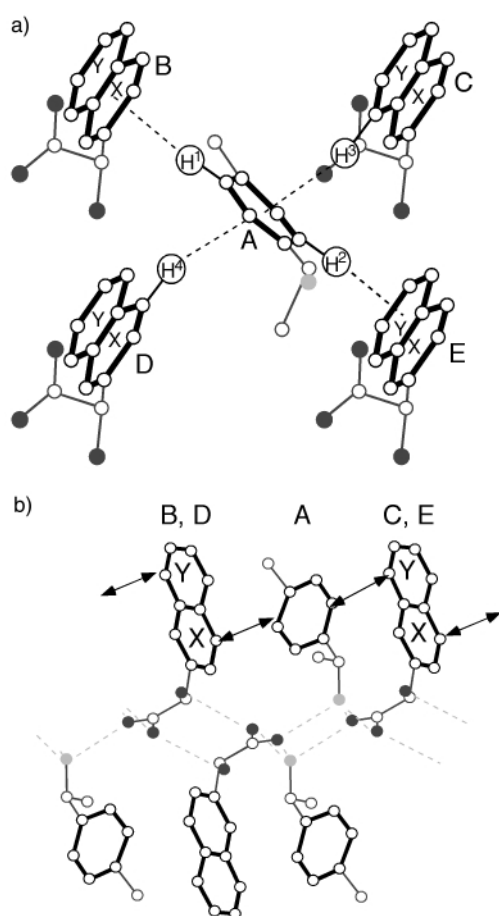


Fig. 4 Packing of the aromatic groups in the supramolecular hydrogen-bond sheets, viewed a) vertically down and b) horizontally across the supramolecular sheet.

ethylamines was considerably enhanced, compared with those of enantiopure mandelic acid and its *p*-substituted derivatives. The designed enantiopure 2-naphthylglycolic acid (**2**) was readily available from a commercially available raw material through simple procedures, and enantiopure **2** showed excellent resolution ability over a wide variety of non-, *m*- and *p*-substituted 1-arylethylamines. X-Ray crystallographic studies on the less- and more-soluble salts have suggested that there exist three

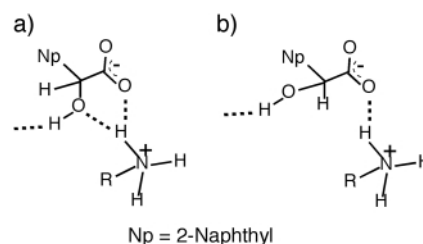


Fig. 5 Schematic representations of a) bifurcated hydrogen bonds commonly found in the less-soluble salts and b) hydrogen bonds found in more-soluble (*S*)-2·(*R*)-3g and (*S*)-2·(*R*)-3k.

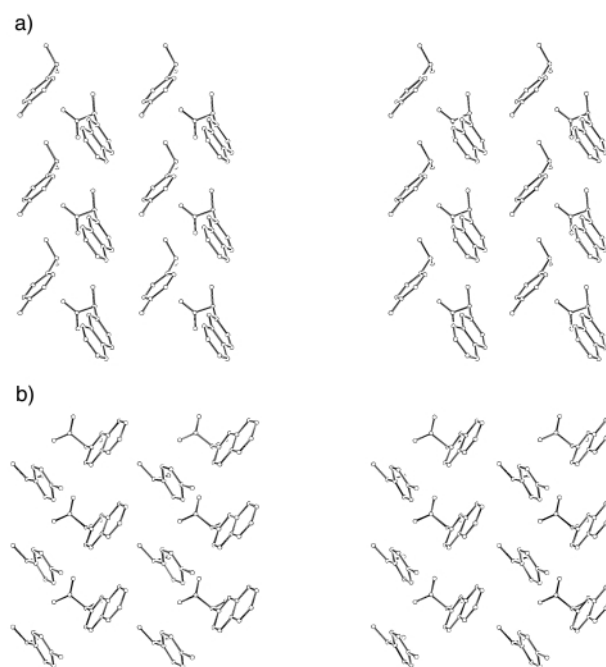


Fig. 6 Stereoview of the packing of the aromatic groups viewed vertically down the supramolecular sheet. The hydrogen atoms are omitted for clarity. a) Less-soluble (*R*)-2·(*R*)-3f. b) More-soluble (*R*)-2·(*S*)-3f.

factors, hydrogen-bonding, $\text{CH}\cdots\pi$, and hydrophobic interactions, for the stabilisation of the crystals of the diastereomeric salts, and the importance of the interaction decreases in this order. The dramatic enhancement in the resolution ability

of enantiopure **2** for 1-arylethylamines would originate from the effective CH $\cdots\pi$ interaction, while the hydrophobic interaction, of which the effectiveness has a high correlation with the relative molecular length between the racemates and the resolving agent, would be less important in the chiral discrimination mechanism. On the other hand, when the target racemates are other types of amines, effective CH $\cdots\pi$ interaction would be absent in the supramolecular sheet, and hence the hydrophobic interaction would become an important factor.

Experimental

General

The IR spectra were recorded on a JASCO IR-810 spectrophotometer, and the $^1\text{H-NMR}$, $^{13}\text{C-NMR}$ spectra were measured on a Varian MERCURY 300 instrument using tetramethylsilane as an internal standard. Analytical HPLC was performed using a Daicel Chiralcel OJ-R (eluent: pH 2 $\text{HClO}_4\text{-CH}_3\text{CN} = 8:2$, detected at 254 nm) or CrownPak CR(+) (eluent: pH 2 HClO_4 or 5% MeOH–pH 2 HClO_4 , detected at 200 nm) column. DSC-TG thermograms were measured on Shimadzu DSC-50 and TG-50 instruments, using an aluminium pellet as a standard, at a scan rate of 5.0 $^\circ\text{C min}^{-1}$. The melting points were measured using a Laboratory Devices Mel-Temp and are uncorrected.

Preparation of α,α -dichloroacetophenone

To a solution of acetophenone (150 g, 0.88 mol) in acetic acid (400 cm^3), chlorine was admitted at such a rate that the temperature did not exceed 55 $^\circ\text{C}$. After 20 h, the reaction mixture was poured onto crushed ice (1 dm^3), and the precipitated solid was collected by filtration and then dried under reduced pressure. Recrystallisation of the solid from hexane–chloroform (300 $\text{cm}^3:70 \text{ cm}^3$) afforded α,α -dichloroacetophenone as colorless crystals (179 g, 85% yield). α,α -Dichloroacetophenone: mp: 80–80.5 $^\circ\text{C}$ (lit.³⁰ 83–84 $^\circ\text{C}$); IR (KBr): $\nu = 1705, 1695, 1510, 810, 745 \text{ cm}^{-1}$; $^1\text{H-NMR}$ (300 MHz, CDCl_3): $\delta = 6.84$ (br s, 1H), 7.56–7.69 (m, 2H), 7.88–8.00 (m, 3H), 8.07–8.10 (dd, $J = 2.5 \text{ Hz}, 5.4 \text{ Hz}$, 1H), 8.63 (d, $J = 1.2 \text{ Hz}$, 1H); $^{13}\text{C-NMR}$: $\delta = 67.85, 124.55, 127.85, 128.55, 128.88, 129.48, 129.84, 131.94, 132.19, 136.04, 185.89$.

Preparation of racemic **2**

To a stirred aqueous solution of sodium hydroxide (6.8 g in 60 cm^3 water) was added α,α -dichloroacetophenone (10.07 g) in small portions so that the temperature did not exceed 55 $^\circ\text{C}$. For the addition, about three hours were required. Stirring was continued for an additional 30 min while the temperature was maintained at 55 $^\circ\text{C}$. Then, the reaction mixture was cooled to 0 $^\circ\text{C}$, and to the mixture was added 12 M hydrochloric acid (100 cm^3). After the liberated solid was extracted with ether (3 \times 150 cm^3), the combined ethereal solutions were dried over magnesium sulfate. Removal of the solvent under reduced pressure gave crude racemic **2** (8.74 g), which was washed with chloroform until pure racemic **2** was obtained (5.9 g, 69% yield). **2**: mp: 163.5–167.0 $^\circ\text{C}$ (lit.¹⁷ 155–156 $^\circ\text{C}$); IR (KBr): $\nu = 3350\text{--}3250, 1690, 1400, 1280, 830 \text{ cm}^{-1}$; $^1\text{H-NMR}$ (300 MHz, $[\text{D}_6]\text{DMSO}$): $\delta = 5.21$ (s, 1H), 6.00 (br s, 1H), 7.50–7.58 (m, 3H), 7.88–7.94 (m, 4H); $^{13}\text{C-NMR}$: $\delta = 72.80, 125.08, 125.63, 126.27, 126.49, 127.78, 127.96, 128.08, 132.78, 132.93, 138.05, 174.30$.

Optical resolution of **2**

To a solution of **2** (16 g, 79 mmol) in ethanol (150 cm^3) was added (*R*)-1-phenylethylamine (*R*-**3a**) (9.6 g, 79 mmol); the mixture was refluxed for 30 min. After slow cooling to room temperature, the mixture was left standing for two days, and the precipitated crystalline salt was collected by filtration (5.24 g). The salt was recrystallised three times from 90% aqueous

ethanol to afford pure (*R*)-**2**·(*R*)-**3a** (3.51 g, 28%). This salt was dissolved in water (40 cm^3), and then the solution was acidified with 3 M hydrochloric acid (50 cm^3). The liberated solid was extracted with ether (4 \times 100 cm^3), and the combined organic extracts were dried over magnesium sulfate. Upon removal of the solvent under reduced pressure, the crude acid was obtained as a white solid (2.2 g), which was purified by recrystallisation from ethanol–chloroform (0.7 $\text{cm}^3:10 \text{ cm}^3$) to afford pure (*R*)-**2** (2.00 g, 25% yield). Enantiomeric excess of (*R*)-**2** was determined by an HPLC analysis on Daicel Chiralcel OJ-R (eluent: pH 2 $\text{HClO}_4\text{-CH}_3\text{CN} = 8:2$). (*R*)-**2**: mp: 160.0–161.0 $^\circ\text{C}$ (lit.¹² 160–161 $^\circ\text{C}$); IR (KBr): $\nu = 3350\text{--}3250, 1690, 1400, 1280, 830 \text{ cm}^{-1}$; $^1\text{H-NMR}$ (300 MHz, $[\text{D}_6]\text{DMSO}$): $\delta = 5.21$ (s, 1H), 6.00 (br s, 1H), 7.50–7.58 (m, 3H), 7.88–7.94 (m, 4H); $^{13}\text{C-NMR}$: $\delta = 72.80, 125.08, 125.63, 126.27, 126.49, 127.78, 127.96, 128.08, 132.78, 132.93, 138.05, 174.30$; $[\alpha]_{\text{D}}^{20} = -145.6$ ($c = 0.98$ in EtOH) [lit.¹² $[\alpha]_{\text{D}}^{21} = -142.2$ ($c = 0.98$ in EtOH)].

(*S*)-Enriched **2** was recovered from the filtrate of the first recrystallisation of the above procedure by treatment with 12 M hydrochloric acid (20 cm^3). To a solution of (*S*)-enriched **2** (11.00 g, 54 mmol) in ethanol (100 cm^3) was added (*S*)-**3a** (6.50 g, 54 mmol); the mixture was refluxed for 30 min. After slow cooling to room temperature, the mixture was left standing overnight, and then the precipitated crystalline salt was collected by filtration. The thus-obtained salt was recrystallised three times from 90% aqueous ethanol to afford pure (*S*)-**2**·(*S*)-**3a** as white crystals (7.3 g, 57%). After this salt was dissolved in water (100 cm^3), the solution was acidified with 3 M hydrochloric acid (80 cm^3). The liberated solid was extracted with ether (5 \times 150 cm^3), and the combined organic extracts were dried over anhydrous magnesium sulfate. Upon removal of the solvent under reduced pressure, the crude acid was obtained as a white solid, which was purified by recrystallisation from ethanol–chloroform (2.5 $\text{cm}^3:30 \text{ cm}^3$) to afford pure (*S*)-**2** (3.67 g, 46% yield). (*S*)-**2**: mp: 162.0–163.5 $^\circ\text{C}$; IR (KBr): $\nu = 3350\text{--}3250, 1690, 1400, 1280, 830 \text{ cm}^{-1}$; $^1\text{H-NMR}$ (300 MHz, $[\text{D}_6]\text{DMSO}$): $\delta = 5.21$ (s, 1H), 6.00 (br s, 1H), 7.50–7.58 (m, 3H), 7.88–7.94 (m, 4H); $^{13}\text{C-NMR}$ (300 MHz, $[\text{D}_6]\text{DMSO}$): $\delta = 72.80, 125.08, 125.63, 126.27, 126.49, 127.78, 127.96, 128.08, 132.78, 132.93, 138.05, 174.30$; $[\alpha]_{\text{D}}^{20} = +144.7$ ($c = 0.98$ in EtOH) [lit.¹³ $[\alpha]_{\text{D}}^{21} = +142.5$ ($c = 0.98$ in EtOH)].

Preparation of racemic amines³¹

Racemic amines **3**, **5**, and **6** were prepared by reductive amination of the corresponding ketones. To a solution of a ketone (40 mmol) in methanol (100 cm^3) was added ammonium acetate (0.5 mol) in one portion at room temperature. After the mixture had been stirred for 15 min, sodium cyanoborohydride (28 mmol) was added to the mixture in one portion at room temperature. After being stirred for two days to one week, 6 M hydrochloric acid (30 cm^3) was added to the reaction mixture. The resulting mixture was washed with diethyl ether (2 \times 50 cm^3), and then the aqueous phase was basified to pH = 10 with potassium hydroxide (*ca.* 0.6 mol). The liberated amine was extracted with dichloromethane (3 \times 50 cm^3), and the combined organic extracts were dried over anhydrous magnesium sulfate. After removal of the solvent under reduced pressure, the crude amine was obtained as a colorless oil, which was further purified by distillation under reduced pressure.

Optical resolution of racemic amines with (*S*)-**2**

To a solution of a racemic amine in aqueous ethanol (the amounts and ratios are summarised in Table 1) was added an equimolar amount of (*S*)-**2**, and the mixture was heated to reflux. The solution was then slowly cooled to 30 $^\circ\text{C}$ and left standing for 12 h in a water bath kept at 30 $^\circ\text{C}$. The precipitated crystalline salt was collected by filtration. The salt was dissolved in water, and the solution was acidified with 3 M hydrochloric acid. After the solution was extracted with ether to recover (*S*)-

2, the aqueous phase was basified to pH = 10 with potassium hydroxide. The liberated oil was extracted with dichloromethane a few times, and the combined organic extracts were dried over anhydrous magnesium sulfate. After removing the solvent under reduced pressure, the amine was obtained as a colorless oil, the enantiomeric excess of which was determined by HPLC on Daicel Chiralcel OJ-R (in the cases of **3b** and **4**), or Daicel CrownPak CR(+) (in the other cases).

Preparation of single crystals

Single crystals for X-ray analysis were prepared by slow evaporation of the solvent from a saturated solution in aqueous ethanol or by slow cooling without evaporation.

(R)-2·(R)-**3a**: mp: 184.0–187.5 °C; $\nu_{\max}/\text{cm}^{-1}$: 3200–2400, 1722, 1695, 1223, 830, 815, and 745; $^1\text{H-NMR}$ (300 MHz, $[\text{D}_6]$ DMSO): δ = 1.43 (d, J = 6.6 Hz, 3H), 2.9–3.8 (br s, 3H), 4.28 (q, J = 6.6 Hz, 1H), 4.71 (s, 1H), 7.42–7.48 (m, 7H), 7.57 (d, J = 8.4 Hz, 1H), 7.78 (d, J = 8.7 Hz, 1H), 7.85 (d, J = 2.7 Hz, 3H).

(S)-2·(S)-**3e**: mp: 168.0–170.0 °C; $\nu_{\max}/\text{cm}^{-1}$: 3300, 3200–2600, 1635, 1610, 1580, 1385, 1075, 795, 755, and 700; $^1\text{H-NMR}$ (300 MHz, $[\text{D}_6]$ DMSO): δ = 1.41 (d, J = 6.6 Hz, 3H), 3.19 (br s, 3H), 3.73 (s, 3H), 4.26 (m, 1H), 4.70 (s, 1H), 6.88 (d, J = 5.7 Hz, 1H), 6.94 (d, J = 21.0 Hz, 1H), 7.05 (s, 1H), 7.28 (t, J = 9.2 Hz, 1H), 7.31–7.47 (m, 2H), 7.56 (d, J = 8.4 Hz, 1H), 7.77 (d, J = 8.1 Hz, 1H), 7.85 (d, J = 3.9 Hz, 3H).

(R)-2·(R)-**3f**: mp: 200.5–208.0 °C; $\nu_{\max}/\text{cm}^{-1}$: 3300–2600, 1640, 1600, 1570, 1530, 1385, 1075, 825, 810, and 745; $^1\text{H-NMR}$ (300 MHz, $[\text{D}_6]$ DMSO): δ = 1.40 (d, J = 6.6 Hz, 3H), 2.27 (s, 3H), 2.9–4.0 (br s, 3H), 4.26 (q, J = 6.6 Hz, 1H), 4.70 (s, 1H), 7.15 (d, J = 7.8 Hz, 2H), 7.30 (d, J = 7.8 Hz, 2H), 7.40–7.48 (m, 2H), 7.56 (d, J = 8.7 Hz, 1H), 7.78 (d, J = 8.1 Hz, 1H), 7.86 (s, 3H).

(R)-2·(S)-**3f**: mp: 154.5–159.5 °C; $\nu_{\max}/\text{cm}^{-1}$: 3400–3200, 3200–2600, 1625, 1560, 1515, 1385, 1245, 1080, 825, and 755; $^1\text{H-NMR}$ (300 MHz, $[\text{D}_6]$ DMSO): δ = 1.40 (d, J = 6.6 Hz, 3H), 2.27 (s, 3H), 2.9–4.0 (br s, 3H), 4.24 (q, J = 6.6 Hz, 1H), 4.68 (s, 1H), 7.15 (d, J = 7.8 Hz, 2H), 7.30 (d, J = 7.8 Hz, 2H), 7.40–7.48 (m, 2H), 7.56 (d, J = 8.7 Hz, 1H), 7.78 (d, J = 8.1 Hz, 1H), 7.86 (s, 3H).

(S)-2·(S)-**3g**: mp: 203.0–209.5 °C; $\nu_{\max}/\text{cm}^{-1}$: 3200–2600, 2600–3200, 1610, 1575, 1530, 1380, 1075, 835, 815 and 765; $^1\text{H-NMR}$ (300 MHz, $[\text{D}_6]$ DMSO): δ = 1.12 (t, J = 7.8 Hz, 3H), 1.41 (d, J = 6.6 Hz, 3H), 2.55 (q, J = 7.8 Hz, 3H), 2.9–4.0 (br s, 3H), 4.23 (q, J = 6.6 Hz, 3H), 4.73 (s, 1H), 7.14 (d, J = 7.8 Hz, 2H), 7.31 (d, J = 7.8 Hz, 2H), 7.41–7.49 (m, 2H), 7.58 (d, J = 8.4 Hz, 1H), 7.78 (d, J = 8.4 Hz, 1H), 7.84–7.86 (m, 3H).

(S)-2·(R)-**3g**: mp: 177.0–181.5 °C; $\nu_{\max}/\text{cm}^{-1}$: 3400–3200, 3200–2600, 1625, 1575, 1525, 1385, 1080, and 765; $^1\text{H-NMR}$ (300 MHz, $[\text{D}_6]$ DMSO): δ = 1.12 (t, J = 7.8 Hz, 3H), 1.41 (d, J = 6.6 Hz, 3H), 2.55 (q, J = 7.8 Hz, 3H), 2.9–4.0 (br s, 3H), 4.23 (q, J = 6.6 Hz, 3H), 4.73 (s, 1H), 7.14 (d, J = 7.8 Hz, 2H), 7.31 (d, J = 7.8 Hz, 2H), 7.40–7.49 (m, 2H), 7.58 (d, J = 8.4 Hz, 1H), 7.78 (d, J = 8.4 Hz, 1H), 7.85–7.86 (m, 3H).

(S)-2·(S)-**3k**: mp: 207.0–212.0 °C; $\nu_{\max}/\text{cm}^{-1}$: 3200–2600, 2550, 1635, 1610, 1560, 1535, 1385, 1075, 835, 815, 770, 750, and 730; $^1\text{H-NMR}$ (300 MHz, $[\text{D}_6]$ DMSO): δ = 1.39 (d, J = 6.6 Hz, 3H), 2.9–4.0 (br s, 3H), 4.30 (q, J = 6.6 Hz, 1H), 4.73 (s, 1H), 7.39–7.48 (m, 7H), 7.56 (d, J = 8.4 Hz, 1H), 7.78 (d, J = 8.4 Hz, 1H), 7.85 (s, 2H).

(S)-2·(R)-**3k**: mp: 176.5–182.0 °C; $\nu_{\max}/\text{cm}^{-1}$: 3400–3200, 3200–2600, 1630, 1575, 1555, 1510, 1385, 1245, 1080, and 765; $^1\text{H-NMR}$ (300 MHz, $[\text{D}_6]$ DMSO): δ = 1.39 (d, J = 6.6 Hz, 3H), 2.8–4.0 (br s, 3H), 4.30 (q, J = 6.6 Hz, 1H), 4.73 (s, 1H), 7.39–7.49 (m, 7H), 7.56 (d, J = 8.4 Hz, 1H), 7.78 (d, J = 8.4 Hz, 1H), 7.85 (s, 2H).

(R)-2·(R)-**3m**: mp: 166.0–167.5 °C; $\nu_{\max}/\text{cm}^{-1}$: 3200–2400, 1615, 1570, 1520, 1385, 1255, 1075, 835, 815, and 750; $^1\text{H-NMR}$ (300 MHz, $[\text{D}_6]$ DMSO): δ = 1.43 (d, J = 6.6 Hz, 3H),

2.9–4.0 (br s, 3H), 3.74 (s, 3H), 4.26 (q, J = 6.6 Hz, 1H), 4.70 (s, 1H), 7.15 (d, J = 7.8 Hz, 2H), 7.30 (d, J = 7.8 Hz, 2H), 7.40–7.48 (m, 3H), 7.56 (d, J = 8.7 Hz, 1H), 7.78 (d, J = 8.1 Hz, 1H), 7.86 (s, 2H).

Crystal structure determination and refinement ¶

The X-ray intensities were measured up to $2\theta = 130^\circ$ with graphite-monochromated Cu-K α radiation ($\lambda = 1.5418 \text{ \AA}$) on a Mac Science MXC18 four-circle diffractometer by a 2θ - ω scan. All of the data were collected at 293 K. The cell dimensions were obtained by least-square analyses of the setting angles of 20 reflections ($50^\circ < 2\theta < 60^\circ$). The intensities and orientation of the crystals were checked by three standard reflections every 100 reflections.

The structures were solved and refined by applying the CRYSTAN-GM package;³² the direct method (SIR92³³) was followed by normal heavy-atom procedures, and full-matrix least-squares refinement with all non-hydrogen atoms anisotropic and hydrogens in calculated positions with thermal parameters equal to those of the atom to which they were bonded.

Acknowledgements

The present work was supported by Grants-in-Aid for Scientific Research (Nos. 09450330 and 10750618) from the Ministry of Education, Science, Sports and Culture of Japan.

¶ CCDC reference number 188/250. See <http://www.rsc.org/suppdata/p2/b0/b000903m/> for crystallographic files in .cif format.

References

- 1 Preliminary communication, see: K. Kinbara, Y. Harada and K. Saigo, *Tetrahedron: Asymmetry*, 1998, **9**, 2219.
- 2 J. Jacques, A. Collet and S. H. Wilen, *Enantiomers, Racemates and Resolutions*; Krieger Publishing Company: Malabar, FL, 1994; A. Collet, *Comprehensive Supramolecular Chemistry*, Vol. **10**, (Ed.: D. N. Reinhoudt), Pergamon, Oxford, 1996, pp. 113–149.
- 3 L. Pasteur, *C. R. Acad. Sci.*, 1853, **37**, 162.
- 4 For examples, see: M. Ács, E. Novotny-Bregger, K. Simon and G. Argay, *J. Chem. Soc., Perkin Trans. 2*, 1992, 2011; E. Fogassy, F. Faigl and M. Ács, *Tetrahedron*, 1993, **41**, 2837; E. J. Ebbers, B. J. M. Plum, G. J. A. Ariaans, B. Kaptein, Q. B. Broxterman, A. Bruggink and B. Zwanenburg, *Tetrahedron: Asymmetry*, 1997, **8**, 4047; E. Ebbers, G. J. A. Ariaans, B. Zwanenburg and A. Bruggink, *Tetrahedron: Asymmetry*, 1998, **9**, 2745.
- 5 S. P. Zingg, E. M. Arnett, A. T. McPhail, A. A. Bothner-By and W. R. Gilkerson, *J. Am. Chem. Soc.*, 1988, **110**, 1565; F. J. J. Leusen, J. H. Noordik and H. R. Karfunkel, *Tetrahedron*, 1993, **49**, 5377.
- 6 For selected examples of the crystallographic studies on the less- and more-soluble diastereomeric salts, see: P. M.-C. Brianso, *Acta Crystallogr., Sect. B*, 1976, **32**, 3040; R. O. Gould and M. D. Walkinshaw, *J. Am. Chem. Soc.*, 1984, **106**, 7840; E. Fogassy, M. Ács, F. Faigl, K. Simon, J. Rohonczy and Z. Ecsery, *J. Chem. Soc., Perkin Trans. 2*, 1986, 1881; E. Fogassy, F. Faigl, M. Ács, K. Simon, É. Kozsda, B. Podányi, M. Czugler and G. Reck, *J. Chem. Soc., Perkin Trans. 2*, 1988, 1385; K. Simon, É. Kozsda, Z. Böcskei, F. Faigl, E. Fogassy and G. Reck, *J. Chem. Soc., Perkin Trans. 2*, 1990, 1395; M. Ács, E. Novotny-Bregger, K. Simon and G. Argay, *J. Chem. Soc., Perkin Trans. 2*, 1992, 2011; S. Larsen, H. L. de Diego and D. Kozma, *Acta Crystallogr., Sect. B*, 1993, **49**, 310; R. Yoshioka, O. Ohtsuki, T. Da-te, K. Okamura and M. Senuma, *Bull. Chem. Soc. Jpn.*, 1994, **67**, 3012; A. Gjerlov and S. Larsen, *Acta Crystallogr., Sect. B*, 1997, **53**, 708; M. R. Cairra, R. Clauss, L. R. Nassimbeni, J. L. Scott and A. F. Wildervanck, *J. Chem. Soc., Perkin Trans. 2*, 1997, 763.
- 7 K. Kinbara, Y. Kobayashi and K. Saigo, *J. Chem. Soc., Perkin Trans. 2*, 1998, 1767; K. Kinbara, Y. Kobayashi and K. Saigo, *J. Chem. Soc., Perkin Trans. 2*, 2000, 111.
- 8 K. Kinbara, K. Sakai, Y. Hashimoto, H. Nohira and K. Saigo, *Tetrahedron: Asymmetry*, 1996, **7**, 1539.
- 9 K. Kinbara, K. Sakai, Y. Hashimoto, H. Nohira and K. Saigo, *J. Chem. Soc., Perkin Trans. 2*, 1996, 2615.

- 10 We have recently found that in the case of the resolution of 2-arylalkanoic acids by enantiopure amino alcohols, the efficiency of resolution was considerably improved by using a rigid resolving agent, see: ref. 7.
- 11 M. Nishio, M. Hirota and Y. Umezawa, *CH $\cdots\pi$ Interaction: Evidence, Nature and Consequences*, Wiley-VCH Publication: Weinheim, Berlin, 1998; F. Toda, K. Tanaka, Z. Stein and I. Goldberg, *J. Org. Chem.*, 1994, **59**, 5748; A. L. Lmas-Saiz, C. Foces-Foces, P. Molina, M. Alajarin, A. Vidal, R. M. Claramunt and J. Elgueno, *J. Chem. Soc., Perkin Trans. 2*, 1991, 1025.
- 12 R. Howe, R. H. Moore and B. S. Rao, *J. Med. Chem.*, 1973, **19**, 1020.
- 13 I. Takahashi, K. Odashima and K. Koga, *Chem. Pharm. Bull.*, 1985, **33**, 3571.
- 14 K. Hattori, K. Takahashi and N. Sakai, *Bull. Chem. Soc. Jpn.*, 1992, **65**, 2690.
- 15 J. G. Aston, J. D. Newkirk, D. M. Jenkins and J. Dorsky, *Org. Synth., Coll. Vol. 3*, John Wiley & Sons, p. 538; T. Sugawara, T. Toyota and K. Sasakura, *Synth. Commun.*, 1979, **9**, 583.
- 16 H. A. Pinner, *Chem. Ber.*, 1891, **24**, 546.
- 17 E. L. Compere, Jr., *J. Org. Chem.*, 1968, **33**, 2565.
- 18 S. K. Latypov, J. M. Seco, E. Quinoa and R. Riguera, *J. Org. Chem.*, 1995, **60**, 504.
- 19 We selected these resolving agents because both their enantiopure forms are available.
- 20 For examples of the resolution of **3k**, see: H. Matsumoto, JP 93-157394; H. Nohira and A. Takebayashi, JP 92-126388; S. Hasegawa and H. Sato, JP 89-128236; G. Gottarelli and B. Samori, *J. Chem. Soc. (B)*, 1971, 2418; T. Manimaran and A. A. Potter, US Patent 5,162,576, 1992.
- 21 For examples of the resolution of **4**, see: R. R. Bottoms, US Patent 3,000,947, 1961; C. W. Den Hollander, W. Leimgruber and E. Mohacsi, US Patent 3,682,925, 1972; M. Nishimura and M. Uya, JP 91-133771.
- 22 For an example of the application of the Schröder–van Laar equation to the diastereomeric mixtures, see: ref. 1.
- 23 A table of N \cdots O and O \cdots O distances in the diastereomeric salts is deposited as supporting information (Table S1).
- 24 Concerning the herringbone packing of aromatic molecules, see: A. Gavezzotti and G. R. Desiraju, *Acta. Crystallogr., Sect. B*, 1988, **44**, 427; G. R. Desiraju and A. Gavezzotti, *Acta. Crystallogr., Sect. B*, 1989, **45**, 473.
- 25 A table of the angles and lengths between the stacking aromatic rings is deposited as supporting information (Table S2).
- 26 For studies concerning the correlation between the strength of a hydrogen bond and an IR absorption band, see: K. Nakamoto, M. Margoshes and R. E. Rundle, *J. Am. Chem. Soc.*, 1955, **77**, 6480; L. P. Kuhn, *J. Am. Chem. Soc.*, 1952, **74**, 2492; L. J. Bellamy and R. J. Pace, *Spectrochim. Acta*, 1969, **25**, 319.
- 27 IR absorption bands related to the hydroxy and carboxylate groups for the less- and more-soluble salts (cm $^{-1}$): less-soluble (*R*)-**2**·(*R*)-**3f** (3290, 1610, 1230), more-soluble (*R*)-**2**·(*S*)-**3f** (3310, 1625, 1245); less-soluble (*S*)-**2**·(*S*)-**3g** (3270, 1610, 1225), more-soluble (*S*)-**2**·(*R*)-**3g** (3330, 1630, 1245); less-soluble (*S*)-**2**·(*S*)-**3k** (3250, 1575, 1380), more-soluble (*S*)-**2**·(*S*)-**3k** (3350, 1635, 1420). In all cases, the absorption bands of the more-soluble salts were shifted upward from those of the corresponding less-soluble salts.
- 28 Theoretical studies suggest that a T-shape geometry ($\theta = 90^\circ$) is the most stable for a benzene dimer.²⁹
- 29 G. Karlström, P. Linse, A. Wallqvist and B. Jönsson, *J. Am. Chem. Soc.*, 1983, **105**, 3777; S. K. Burley and G. A. Petsko, *J. Am. Chem. Soc.*, 1986, **108**, 7995; C. A. Hunter and J. K. M. Sanders, *J. Am. Chem. Soc.*, 1990, **112**, 5525.
- 30 I. R. Zubkowski, *Chem. Zentralbl., II*, 1929, 2775.
- 31 R. F. Borch, M. D. Bernstein and H. D. Durst, *J. Am. Chem. Soc.*, 1971, **93**, 2897.
- 32 CRYSTAN GM, a computer program for the solution and refinement of crystal structures for X-ray diffraction data (Mac Science Corporation).
- 33 A. Altomare, G. Cascarano, C. Giacovazzo and A. Guagliardi, *J. Appl. Crystallogr.*, 1993, **26**, 343.